JOURNAL OF SOLID STATE CHEMISTRY **135,** 52–58 (1998)
ARTICLE NO. SC977589

# Structural Disorder in Mechanosynthesized Zinc Ferrite

V. Šepelák,* U. Steinike,† D. Chr. Uecker,† S. Wißmann,‡ and K. D. Becker‡

*Institute of Geotechnics of the Slovak Academy of Sciences, 04353 Košice, Slovakia; †Institute of Applied Chemistry e.V., 12484 Berlin, Germany; and ‡Institute of Physical and Theoretical Chemistry, Technical University of Braunschweig, 38106 Braunschweig, Germany

Received May 9, 1997; in revised form August 10, 1997; accepted August 11, 1997

**The character of the mechanically induced structural disorder and nature of the metastability of mechanosynthesized zinc ferrite are elucidated by investigation of its structure. Attention is concentrated on the explanation of an origin of mechanically induced changes in magnetic properties of the nanoscale mechanosynthesized ferrite. The range of thermal stability of mechanically induced metastable states is determined by studying the response of the metastable mechanosynthesized zinc ferrite to changes in temperature.** © 1998 Academic Press

*Key Words:* **Mechanosynthesis; spinel; zinc ferrite; mechanically induced disorder; metastable material.**

## 1. INTRODUCTION

The synthesis of inorganic compounds is a fundamental problem in chemistry and chemical engineering. The idea of using solid-state reactions to avoid dissolving steps, fusion, or sintering of the reactants in the course of synthesis has always been attractive. However, inadequate mixing of the reaction components, low contact surface, and strong diffusion resistance make the application of solid-state reaction difficult. The formation of complex oxides with the spinel structure using the conventional solid-state reaction between simple oxides proceeds especially slowly and requires prolonged exposure at considerably elevated temperatures (1–4).

New methods of material synthesis have received increased attention in recent years. Of particular interest are low-temperature techniques, such as room-temperature ball-milling, which offer the possibility of forming structures exhibiting new and unusual properties. Although the mechanochemical synthesis is of great interest in solid-state physics, chemistry, and material science and has been applied to a wide range of solids (5–7), we found only a few papers in the literature on the application of the high-energy $\infty$ ball-milling to synthesize a spinel ferrite (8–18).

The mechanochemical route for the preparation of magnetite has been reported (8, 9). The hematite to magnetite chemical reduction has been achieved by wet-milling of $\alpha$-$Fe_2O_3$ in oxygen-free conditions.

It has been revealed that ball-milling is a suitable technique for the preparation of nanocrystalline nickel ferrite staring from NiO and $\alpha$-$Fe_2O_3$ powders in equimolar ratio (10). Compacts of nickel ferrite obtained by reaction sintering of powders mechanically treated for various times exhibit remarkably different specific electric resistivity.

The synthesis of ferrite with the spinel structure by the direct mechanochemical interaction has been observed by the investigation of the products of the reactions $MeO + Fe_2O_3 \rightarrow MeFe_2O_4$, where $Me =$ Cd and Ca (11).

The investigation of the influence of mechanical activation of the $\alpha$-$Fe_2O_3$/ZnO mixture on the formation of zinc ferrite has revealed that it is possible to achieve the mechanosynthesis of zinc ferrite from zinc oxide and iron oxide powders at room temperature in a planetary mill (11–15).

In our previous papers (16, 17), we studied the surface structure of mechanosynthesized zinc ferrite by X-ray photoelectron spectroscopy. The results of the surface analytical studies revealed that the surface structure of mechanosynthesized zinc ferrite corresponds to the structure of the inverse spinel.

One of the most promising applications of mechanosynthesized zinc ferrite is its use as an absorbent material in high-temperature coal gas desulfurization. Results of the sulfurization tests, reported in our previous work (18), have revealed that interaction of mechanosynthesized zinc ferrite with the components of coal gas ($H_2S$, CO, $H_2$) results in the most apparent increase of the sulfur absorption capacity when compared with the reactivity of the unmilled $\alpha$-$Fe_2O_3$/ZnO mixture as well as with the reactivity of the ball-milled zinc ferrite that was prepared by the conventional thermal method (18, 19). In spite of this favorable effect of the mechanochemical preparation route on the reactivity of zinc ferrite, little is known of the structural state of this solid.

It should be emphasized that the literature which deals with the mechanosynthesis of spinel ferrites is not broad, and the investigation of the mechanically induced structural



0022-4596/98 $25.00

disorder and studies of the basic physical and chemical properties of mechanosynthesized spinel ferrites are so far missing. In most of the aforementioned papers, only the formation of mechanosynthesized spinel ferrite has been established by X-ray diffraction and Mössbauer spectroscopy. Not much has been determined on the defect state or structure of spinel ferrites prepared by unconventional mechanochemical routes. Another problem, which was studied only to a limited extent until now, is related to the thermal stability of mechanically induced structural defects in these solids.

The aim of the present work is to elucidate the character of mechanically induced structural disorder and the nature of metastability of the mechanosynthesized zinc ferrite as well as to determine the range of thermal stability of the mechanically induced metastable states in this solid.

## 2. EXPERIMENTAL

The mechanochemical route was used for the preparation of zinc ferrite. Stoichiometric mixtures of powdered reactants containing 66.34% $\alpha$-$Fe_2O_3$ and 33.76% ZnO by weight (products of Merck) were used as starting materials. The milling process was carried out in an AGO 2 planetary ball mill (Institute of Solid State Chemistry, Novosibirsk) at room temperature. Ten grams of the starting material was sealed in a stainless steel vial (150 $cm^3$ in volume) together with stainless steel balls 5 mm in diameter. The ball to powder weight ratio was 20 : 1. Milling experiments were performed in air at 800 rpm.

X-ray diffraction (XRD) patterns were collected using a URD 6 powder diffractometer (Seifert-FPM, Freiberg) with Cu$K\alpha$ or Co$K\alpha$ radiation. Data interpretation was carried out using the JCPDS database. The XRD analysis was pursued with the STADI P software (Stoe, Darmstadt). *In situ* X-ray diffraction analysis was performed in a Guinier–Lennè camera (Enraf–Nonius, Delft) as well as in an XRK-A Paar camera (A Paar GmbH, Graz) at a heating rate of 2 K $min^{-1}$ over the temperature range 300–1100 K.

Scanning electron microscopy (SEM) (Model BS-300, Tesla, Brno) was used to observe the morphology of the powder and the individual particle size. The particle size distribution was measured by laser radiation scattering using the Laser-Particle-Sizer Analysette 22 granulometer (Fritsch, Idar-Oberstein). The mean particle diameter was calculated from granulometric data. The specific surface area was determined by the standard Brunauer–Emmett–Teller (BET) method using the Gemini 2360 apparatus (Sy-Lab, Vienna).

Mössbauer spectroscopy experiments were performed in transmission geometry using a conventional microcomputer-controlled spectrometer in constant acceleration mode. A $^{57}$Co/Rh $\gamma$-ray source was used. The velocity scale was calibrated relative to $\alpha$-Fe. A proportional counter was used to detect the transmitted $\gamma$-rays. The spectra were fitted by the least-squares minimization method (20).

## 3. RESULTS AND DISCUSSION

The mechanically induced evolution of the $Fe_2O_3$/ZnO mixture submitted to the high-energy ball-milling process was followed by $^{57}$Fe Mössbauer spectroscopy. This method is sensitive to the structural environment of iron atoms on a short (essentially nearest neighbor) length scale and is therefore able to provide information on the structural state of mechanosynthesized zinc ferrite.

Mössbauer spectroscopy measurements revealed that the room-temperature Mössbauer spectrum of the starting $Fe_2O_3$/ZnO mixture consists of a hyperfine sextet corresponding to the magnetically ordered $\alpha$-$Fe_2O_3$; see Fig. 1a. With increasing milling time, the hyperfine magnetic sextet in the spectrum disappears and is gradually replaced with a paramagnetic doublet (Figs. 1b–d) with isomer shift IS = 0.331 mm $s^{-1}$ and quadrupole splitting QS = 0.433 mm $s^{-1}$ characteristic of $ZnFe_2O_4$ (21–24). Thus, the Mössbauer data clearly show that ball-milling of $Fe_2O_3$/ZnO results in the formation of a complex oxide with a spinel structure. We notice that the paramagnetic component assigned to zinc ferrite is visible after 5 min of milling. Further milling leads to a progressive mechanosynthesis of zinc ferrite manifested by the gradual increase of the relative weight of the paramagnetic component in the center of the Mössbauer spectrum. As can be seen, the mechanical treatment leads also to a considerable broadening of the doublet (up to $\Gamma = 0.70$ mm $s^{-1}$) when compared with the crystalline zinc ferrite that was prepared by the conventional ceramic method ($\Gamma = 0.308$ mm $s^{-1}$) (21–24). The broadening of the doublet provides clear evidence of considerable changes in the quadrupolar interaction and indicates the presence of a wide distribution of electric field gradients at the $Fe^{3+}$ nuclei. The large extension of the wings of the signal and weak indications of magnetic structure in the spectrum clearly show that in the activated material some form of magnetic interaction is present. The superposition of the magnetic and quadrupole interactions and the broadening appearing in the spectra at room temperature cannot be resolved by lineshape fitting. Only at lower temperatures do these indications of magnetic interactions become more visible; see Fig. 2 and the discussion of the spectra of mechanosynthesized zinc ferrite at 77 K in the next section. However, the superposition of the magnetic and quadrupole interactions detected in the Mössbauer spectra at room temperature can be attributed to the disordered structure of mechanosynthesized zinc ferrite.

In our previous work (25–28), the crystal structure of the ball-milled zinc ferrite (synthesized by the conventional thermal method and followed by mechanical treatment in

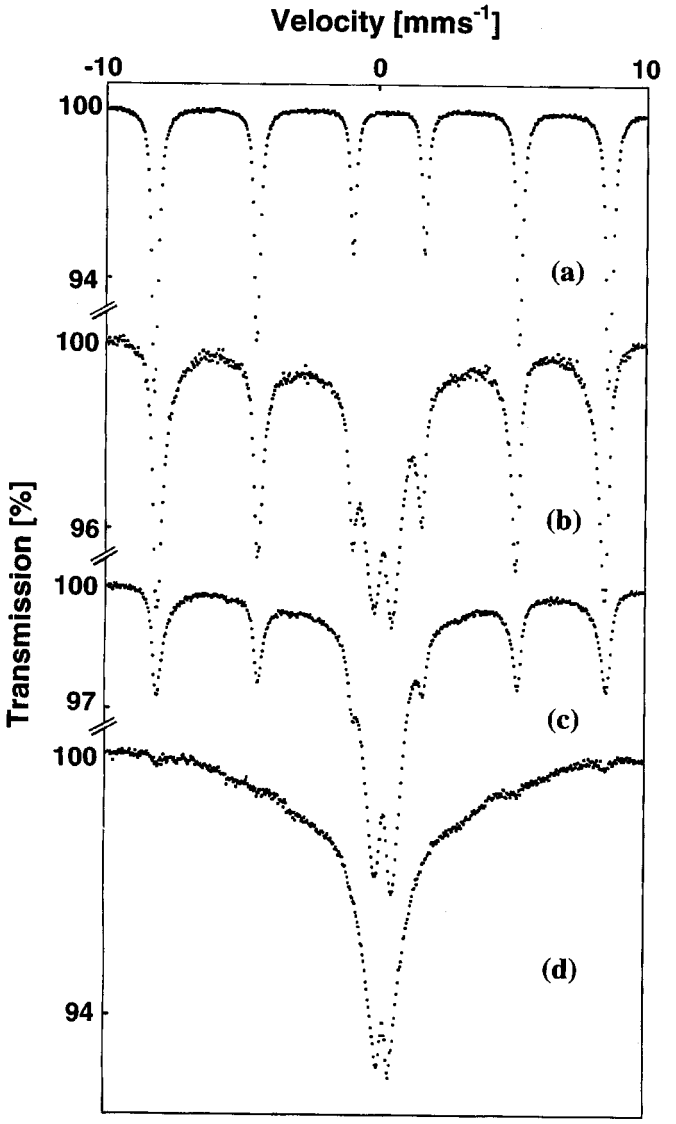


**FIG. 1.** Mössbauer spectra of (a) the starting $Fe_2O_3$/ZnO mixture, (b) the $Fe_2O_3$/ZnO mixture ball-milled for 8 min, (c) the $Fe_2O_3$/ZnO mixture ball-milled for 18 min, and (d) the end product of the ball-milled $Fe_2O_3$/ZnO mixture (mechanosynthesized zinc ferrite) after milling for 120 min.

a planetary ball-mill) was studied using Mössbauer spectroscopy. Comparison of the room-temperature Mössbauer spectra for the mechanosynthesized zinc ferrite and for the ball-milled zinc ferrite revealed that parameters of the Mössbauer spectrum of mechanosynthesized zinc ferrite are close to those of the ball-milled zinc ferrite (25–28). It indicates that the nuclear interactions in the structure of mechanosynthesized zinc ferrite are similar to those of the mechanically treated zinc ferrite.

Information on the structure of mechanosynthesized zinc ferrite obtained by Mössbauer spectroscopy at room

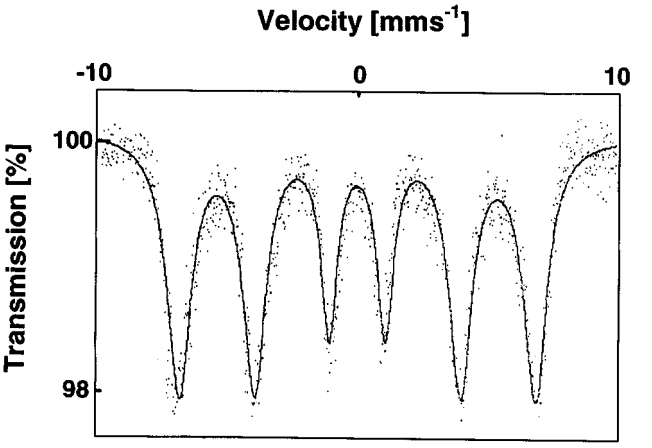


**FIG. 2.** Mössbauer spectrum of mechanosynthesized zinc ferrite taken at 77 K.

temperature was complemented with measurements at liquid nitrogen temperature. An interesting observation is that the Mössbauer spectrum of mechanosynthesized zinc ferrite taken at liquid nitrogen temperature consists of a sextet typical of the magnetically ordered state of the structure, see Fig. 2. It is worth mentioning here that crystalline zinc ferrite (prepared by the conventional thermal method) undergoes a transition from the paramagnetic to a magnetically ordered state at 9 K (29–31). The appearance of the magnetic splitting (IS $= 0.338$ mm s$^{-1}$, hyperfine magnetic field $H = 470$ kG) in the Mössbauer spectrum of mechanosynthesized zinc ferrite at 77 K is therefore a quite unexpected result.

However, it should be emphasized that an identical sextet was observed at liquid nitrogen temperature also in the Mössbauer spectrum of the ball-milled zinc ferrite (synthesized by the conventional thermal method followed by mechanical treatment in a planetary ball-mill) (25–28, 32–35). Thus, the parameters of the Mössbauer spectra of mechanosynthesized zinc ferrite are the same as those of the ball-milled zinc ferrite not only at room temperature but also at liquid nitrogen temperature.

Taking into account the similarity of the hyperfine interactions in the structure of mechanosynthesized zinc ferrite and of the ball-milled zinc ferrite, we have tried to elucidate the character of mechanically induced structural disorder and the nature of metastability of the mechanosynthesized zinc ferrite in analogy with the ball-milled zinc ferrite.

It is well known that zinc ferrite prepared by the conventional thermal method adopts the normal spinel structure, in which the diamagnetic $Zn^{2+}$ cations occupy (A) sites tetrahedrally coordinated by oxygen while the octahedrally coordinated [B] sites are occupied by the $Fe^{3+}$ cations (29–31). According to the Néel theory (36) of ferrimagnetism, there are, in addition to the dominant

antiferromagnetic coupling between magnetic ions on tetrahedral sites and those on octahedral sites, weaker (A)–(A) and [B]–[B] interactions. Since the (A)–[B] coupling is absent in zinc ferrite, this compound exhibits antiferromagnetism at sufficiently low temperatures.

To interpret the presence of magnetic spin arrangements in mechanosynthesized zinc ferrite observed by Mössbauer spectroscopy at 77 K, the results of the Mössbauer spectroscopy studies and of Rietveld analysis of the X-ray and neutron diffraction data of the ball-milled zinc ferrite, reported in our previous work (25–28, 37–39), should be taken into consideration. From these results it was concluded that the mechanical treatment of $ZnFe_2O_4$ results in a substantial displacement of $Zn^{2+}$ cations to octahedral sites and of $Fe^{3+}$ cations into tetrahedral sites of the cubic close-packed anionic sublattice (i.e., mechanically induced inversion takes place). This considerable change is accompanied by a decrease of both unit cell dimension and oxygen parameter. It was also found that the mechanically induced lattice contraction causes the alteration of the octa/cation–anion–octa/cation bond angle.

It is known that the presence of cations with nonzero magnetic moment on the tetrahedral as well as on the octahedral sublattice of spinel ferrites may cause an exchange interaction of the (A)–$O^{2-}$–[B] type. In the mechanosynthesized zinc ferrite, the induced redistribution of $Zn^{2+}$ and $Fe^{3+}$ cations, leading to a substantial inversion of its spinel structure, brings about the onset of the $Fe^{3+}$(A)–$O^{2-}$–$Fe^{3+}$[B] interactions.

The magnetic properties of mechanosynthesized $ZnFe_2O_4$ are also closely connected with the mechanically induced changes of geometrical factors in its structure. Therefore, another factor determining the modified magnetic properties of mechanosynthesized $ZnFe_2O_4$ may be related with the change in the octahedron geometry. The alteration of the octa/cation–anion–octa/cation bond angles leads to the onset of the $Fe^{3+}$[B]–$O^{2-}$–$Fe^{3+}$[B] interaction with deformed bond angles different from 90° (typical for the crystalline zinc ferrite prepared by the conventional thermal method).

Thus, in analogy with the structure of the ball-milled zinc ferrite, we attribute the formation of magnetic spin arrangements in the mechanosynthesized $ZnFe_2O_4$ observed by Mössbauer spectroscopy at 77 K either to the onset of intersublattice exchange interaction of the $Fe^{3+}$(A)–$O^{2-}$–$Fe^{3+}$[B] type (with a bond angle of 125°) taking place due to the mechanically induced inversion or/and to the onset of intrasublattice exchange interactions of the $Fe^{3+}$[B]–$O^{2-}$–$Fe^{3+}$[B] type with deformed bond angles different from 90°.

The mechanochemical reaction was also followed by X-ray powder diffraction. The XRD pattern of the starting powder (Fig. 3a) is characterized by sharp crystalline peaks corresponding to ZnO (JCPDS 36-1451) and $\alpha$-$Fe_2O_3$ (JCPDS 33-664). During the early stages of milling, XRD reveals only a decrease of the intensity and an associated broadening of the Bragg peaks of the individual oxides. With increasing milling time, the weak diffraction lines of both phases completely disappear and the strongest diffraction lines gradually merge together producing a few broad peaks. Moreover, new peaks of $ZnFe_2O_4$ (JCPDS 22-1012) are formed. The broad shape of the diffraction lines assigned to the spinel phase reflects the formation of the disordered structure with the small crystallite size and with the internal strain introduced during the mechanical treatment (compare Figs. 3b and 3c). From line-broadening analysis, the crystallite size in the produced $ZnFe_2O_4$ powder was estimated to be 15 nm. The estimated crystallite size is in good agreement with that observed from the transmission electron microscopy images and reported in our previous work (12, 13). Thus, as the result of a mechanochemical reaction, nanocrystalline $ZnFe_2O_4$ was obtained.

It is worth noting the interesting consideration of several authors (40–42) who studied the magnetic properties of $ZnFe_2O_4$ ultrafine particles ($\sim$10 nm) prepared by a coprecipitation method. They reported that magnetization of $ZnFe_2O_4$ ultrafine particles is extraordinary large compared with that of bulk materials. This fact has also been interpreted by the idea that a fairly large number of $Fe^{3+}$ ions occupy A sites and form magnetic clusters with nearest $Fe^{3+}$ neighbors at B sites through coupling by the A–B interaction. As has been remarked, the number of these clusters would increase with decreasing particle size because cation substitution is pronounced in smaller particles. Taking into account the nanoscale nature of mechanosynthesized zinc ferrite determined by XRD and TEM, it could be assumed that similar magnetic clusters are formed in the course of mechanochemical preparation of zinc ferrite.

The morphology of mechanosynthesized zinc ferrite powders is shown in Fig. 4. The sizes of the powder particles of the starting $Fe_2O_3$/ZnO mixture varied from 10 μm to 20 μm, and the specific surface was 4.8 $m^2\,g^{-1}$. In the course of milling, the powder particles were subjected to a continuous fragmentation. As the result of mechanochemical reaction, the powders become much finer and uniform in shape. While the starting $Fe_2O_3$/ZnO mixture consisted predominantly of individual particles, the sample of mechanosynthesized zinc ferrite consists of aggregates of fine particles. Aggregation was observed by SEM (Fig. 4). Stable aggregates behave under condition of particle size analysis as individual particles and thus the "real" mean particle diameter is smaller than the determined value, $d_m = 1$ μm. The specific surface area of the powders obtained was 10.9 $m^2\,g^{-1}$.

Since the mechanosynthesized solids are metastable with respect to structural and compositional changes under temperature, pressure, and environmental conditions in which they are utilized, there is great concern for understanding and controlling their limitations. Therefore, in addition to

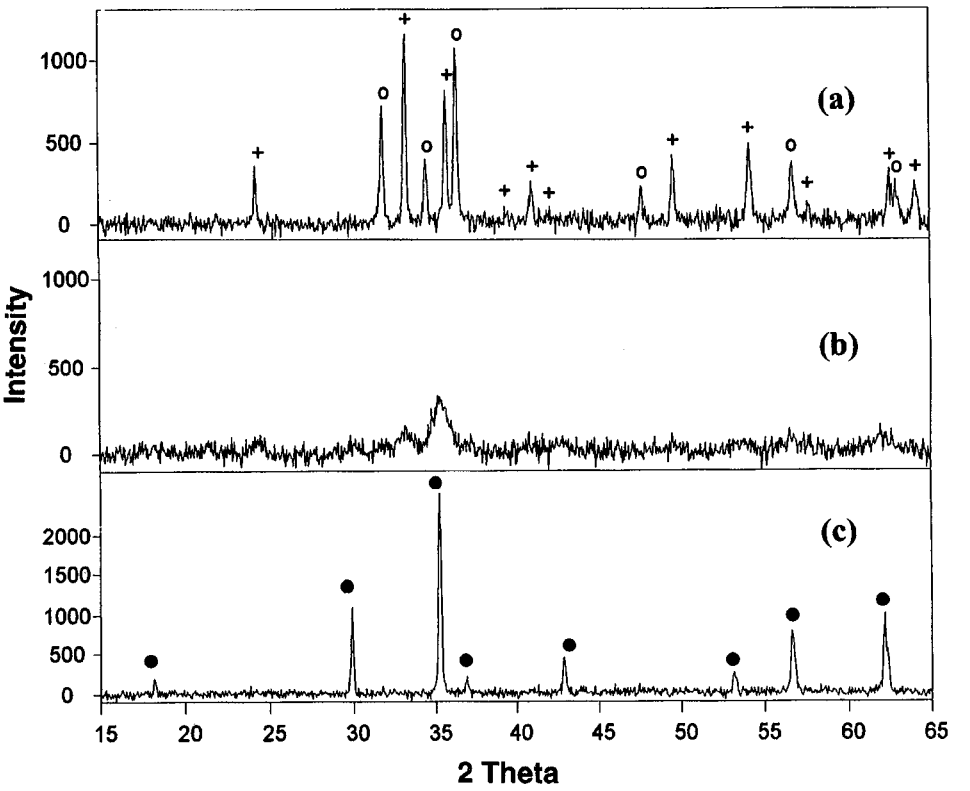


**FIG. 3.** X-ray diffraction patterns of (a) the starting $Fe_2O_3$/ZnO mixture, (b) the mechanosynthesized zinc ferrite, and (c) the crystalline zinc ferrite prepared by the conventional ceramic method. Symbols are (+) $\alpha$-$Fe_2O_3$, (○) ZnO, and (●) $ZnFe_2O_4$ (Cu$K\alpha$ radiation).

study of the mechanically induced disorder, also investigation of the thermal stability of mechanically induced metastable states is necessary.

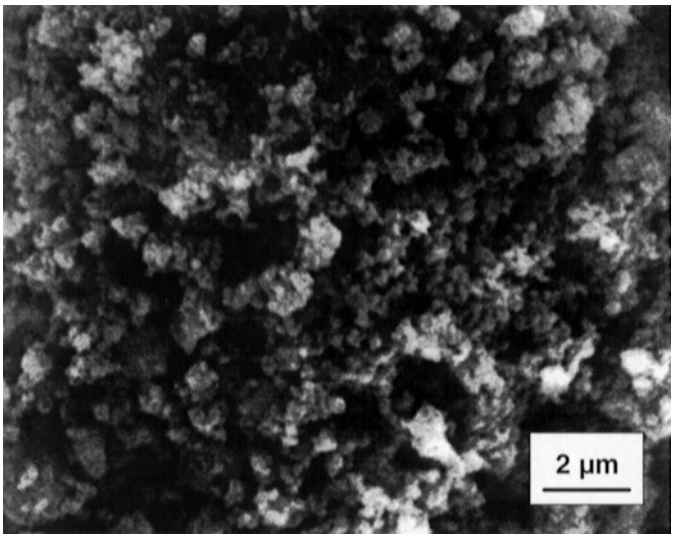


**FIG. 4.** Scanning electron micrograph of mechanosynthesized zinc ferrite.

To compare the thermally induced structural evolution of the starting $Fe_2O_3$/ZnO mixture with changes occurring during the heating of the mechanosynthesized zinc ferrite, *in situ* X-ray diffraction was employed at elevated temperatures using an XRK-A Paar camera and a Guinier–Lennè camera.

As clearly shown in Figs. 5 and 7a, the structural response of the unmilled $Fe_2O_3$/ZnO mixture to changes in temperature is accompanied by an appearance of the sharp crystalline lines of zinc ferrite only at $\sim 1000$ K.

High-temperature XRD analysis revealed that over the range from 293 to 700 K the shape of the diffraction patterns of mechanosynthesized zinc ferrite remains the same, i.e., the interval of the thermal stability of the mechanically induced defects in the structure of mechanosynthesized zinc ferrite is up to 700 K. At temperatures over 700 K the formation of the crystalline zinc ferrite takes place. The crystallization of the nanoscale zinc ferrite terminating at 1100 K is manifested by a gradual narrowing of diffraction lines and by an increase of their intensities, as shown in Figs. 6 and 7c.

It was also found that crystallization of a partly mechanosynthesized zinc ferrite (Fig. 7b) occurs at temperatures which are about 200 K lower than those at which the

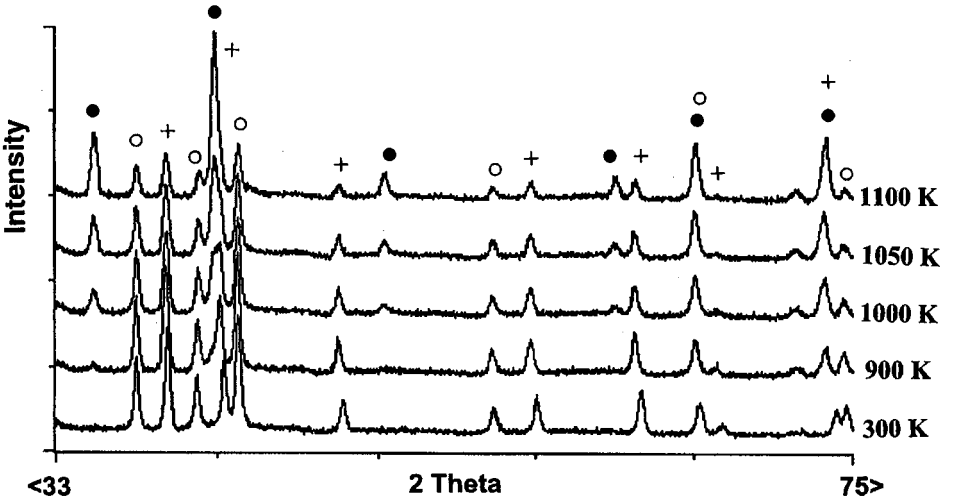


**FIG. 5.** X-ray diffraction patterns of the starting $Fe_2O_3$/ZnO mixtures taken during their thermal treatment in the XRK-A Paar camera (Co$K\alpha$ radiation). Symbols are (+) $\alpha$-$Fe_2O_3$, (○) ZnO, and (●) $ZnFe_2O_4$.

crystalline zinc ferrite is synthesized by the conventional ceramic method. The decrease in synthesis temperature of zinc ferrite can be explained by the effect of sample activation by its mechanical pretreatment, which accelerates the solid phase diffusion processes.

## 4. CONCLUSIONS

The ball-milling of the $Fe_2O_3$/ZnO mixture in a planetary mill results in the formation of nanocrystalline zinc ferrite. The results obtained in this work indicate that the structure of the nanoscale mechanosynthesized zinc ferrite is identical to that of the ball-milled zinc ferrite (synthesized by the conventional ceramic method, followed by mechanical treatment). The metastable structural state of mechanosynthesized zinc ferrite is characterized by a substantial displacement of $Fe^{3+}$ cations to tetrahedral sites and of $Zn^{2+}$ cations into octahedral sites of the cubic close-packed anionic sublattice as well as by the deformation of octahedron geometry. Nuclear hyperfine interactions in the structure of mechanosynthesized zinc ferrite are quite different from those of the crystalline zinc ferrite prepared by the conventional thermal method. The formation of the spin arrangements in the mechanosynthesized $ZnFe_2O_4$ may be attributed either to the onset of intersublattice exchange interaction of the $Fe^{3+}$(A)–$O^{2-}$–$Fe^{3+}$[B] type taking place due to the mechanically induced inversion or/and to the onset of intrasublattice exchange interactions of the $Fe^{3+}$[B]–$O^{2-}$–$Fe^{3+}$[B] type with deformed bond angles. Complex structural changes in mechanosynthesized zinc ferrite cause its transition into a metastable state. The interval of the thermal stability of the mechanically induced

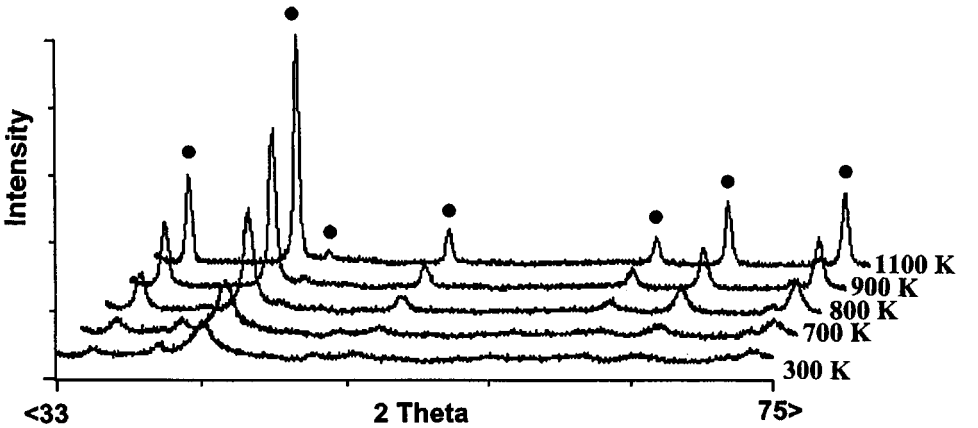


**FIG. 6.** X-ray diffraction patterns of mechanosynthesized zinc ferrite taken during its thermal treatment in the XRK-A Paar camera (Co$K\alpha$ radiation). Diffraction lines of zinc ferrite are indicated by full circles.

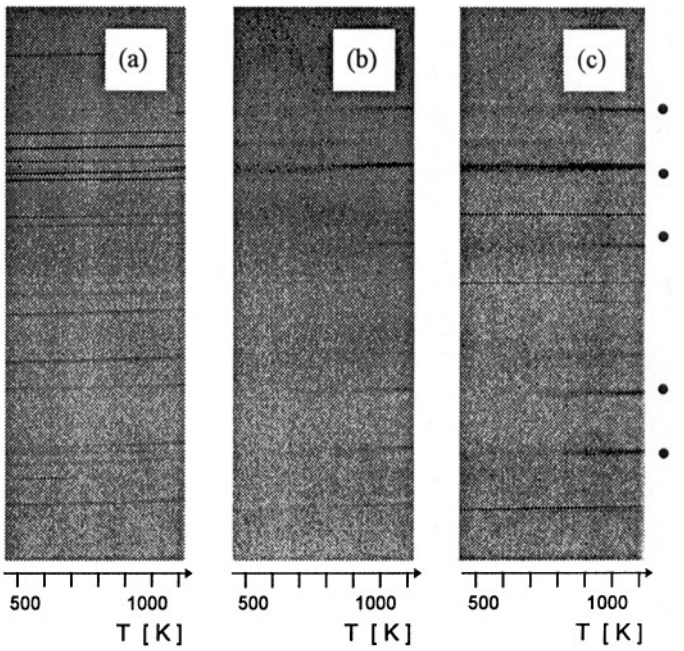


**FIG. 7.** *In situ* XRD analysis of the $Fe_2O_3$/ZnO mixtures during their thermal treatment in a Guinier–Lennè camera: (a) unmilled and (b) ball-milled for 8 min (the partly mechanosynthesized zinc ferrite; ~30 wt.% $ZnFe_2O_4$). (c) Crystallization of mechanosynthesized zinc ferrite during continuous heating. Positions of the diffraction lines of zinc ferrite are indicated by full circles.

defects in the structure of mechanosynthesized zinc ferrite is up to 700 K. Crystallization of the disordered mechanosynthesized zinc ferrite occurs at temperatures which are about 300 K lower than those at which the crystalline zinc ferrite is synthesized by the conventional thermal method.

## ACKNOWLEDGMENTS

This work was supported by the Deutsche Forschungsgemeinschaft (projects 436 SLK 113/1/2 and Ste 692/2-1). The authors are indebted to Professor V. V. Boldyrev for his supporting interest in their work. Special thanks are due to Mr. J. Richter-Mendau for the SEM measurements and Mr. L. Wilde for the *in situ* XRD measurements.

## REFERENCES

1. H. Schmalzried, "Chemical Kinetics of Solids." Verlag Chemie, Weinheim, 1995.
2. R. J. Hill, J. R. Craig, and G. V. Gibs, *Phys. Chem. Miner.* **4,** 317 (1979).
3. A. Navrotsky and O. Kleppa, *J. Inorg. Nucl. Chem.* **30,** 479 (1968).
4. H. Schmalzried, "Solid State Reactions." Verlag Chemie, Weinheim, 1981.
5. M. Magini and D. Fiorani, "Synthesis and Properties of Mechanically Alloyed and Nanocrystalline Materials." Trans Tech Publications, Zürich, 1997.
6. C. Suryanarayana, "Bibliography on Mechanical Alloying and Milling." Cambridge Interscience Publishing, Cambridge, 1995.
7. V. V. Boldyrev, "Reactivity of Solids: Past, Present and Future." Blackwell Science, Oxford, 1996.
8. W. A. Kaczmarek and S. J. Campbell, *Bull. Magn. Reson.* **17,** 148 (1996).
9. W. A. Kaczmarek and B. W. Ninham, *IEEE Trans. Magn.* **MAG-30,** 732 (1994).
10. Č. Jovalekić, M. Zdujić, A. Radaković, and M. Mitrić, *Mater. Lett.* **24,** 365 (1995).
11. G. R. Karagedov and E. A. Konovalova, *in* "Proceedings of the First International Conference on Mechanochemistry, Part 2" (K. Tkáčová, Ed.), p. 70. Cambridge Interscience Publishing, Cambridge, 1994.
12. V. Šepelák, A. Yu. Rogachev, U. Steinike, D. Chr. Uecker, F. Krumeich, S. Wißmann, and K. D. Becker, *Mater. Sci. Forum* **235–238,** 139 (1997).
13. V. Šepelák, A. Yu. Rogachev, U. Steinike, D. Chr. Uecker, S. Wißmann, and K. D. Becker, *Acta Crystallogr., Suppl. Issue A* **52,** C-367 (1996).
14. N. Lefelshtel, S. Nadiv, I. J. Lin, and Y. Zimmels, *Powder Technol.* **20,** 211 (1978).
15. I. J. Lin and S. Nadiv, *Mater. Sci. Eng.* **39,** 193 (1979).
16. P. Druska, D. Chr. Uecker, V. Šepelák, and U. Steinike, *Z. Kristallogr., Suppl. Issue* **12,** 203 (1997).
17. U. Steinike, D. Chr. Uecker, B. Wallis, and V. Šepelák, *Chemical Pap.* in press.
18. V. Šepelák, U. Steinike, D. Chr. Uecker, R. Trettin, S. Wißmann, and K. D. Becker, *Solid State Ionics*, in press.
19. V. Šepelák, K. Jancke, J. Richter-Mendau, U. Steinike, D. Chr. Uecker, and A. Yu. Rogachev, *Kona* **12,** 87 (1994).
20. G. Le Caër and J. M. Dubois, *J. Phys. E* **12,** 1083 (1979).
21. F. Menil, *J. Phys. Chem. Solids* **46,** 763 (1985).
22. A. Hudson and H. J. Whitfield, *Mol. Phys.* **12,** 165 (1967).
23. B. J. Evans, S. S. Hafner, and H. P. Weber, *J. Chem. Phys.* **55,** 5282 (1971).
24. H. St. C. O'Neill, *Eur. J. Miner.* **4,** 571 (1992).
25. V. Šepelák, S. Wißmann, and K. D. Becker, *J. Mater. Sci.*, in press.
26. V. Šepelák, K. Tkáčová, V. V. Boldyrev, and U. Steinike, *Mater. Sci. Forum* **228–231,** 783 (1996).
27. V. Šepelák, M. Zatroch, K. Tkáčová, P. Petrovič, S. Wißmann, and K. D. Becker, *Mater. Sci. Eng A*, in press.
28. V. Šepelák, K. Tkáčová, V. V. Boldyrev, S. Wißmann, and K. D. Becker, *Physica B* **234–236,** 617 (1997).
29. J. M. Hastings and L. M. Corliss, *Phys. Rev.* **102,** 1460 (1956).
30. F. K. Lotgering, *J. Phys. Chem. Solids* **27,** 139 (1966).
31. M. K. Fayek, J. Leciejewiecz, A. Murasik, and I. I. Yamsin, *Phys. Status Solidi* **37,** 843 (1970).
32. Yu. T. Pavlyukhin, Ya. Ya. Medikov, and V. V. Boldyrev, *J. Solid State Chem.* **53,** 155 (1984).
33. Yu. T. Pavlyukhin, Ya. Ya. Medikov, and V. V. Boldyrev, *Mater. Res. Bull.* **18,** 1317 (1983).
34. A. E. Ermakov, E. E. Yurchikov, E. P. Elsukov, V. A. Barinov, and Yu. T. Chukalkin, *Fiz. Tverd. Tela* **24,** 1947 (1982).
35. A. I. Rykov, Yu. T. Pavlyukhin, and Ya. Ya. Medikov, *Proc. Indian Natl. Sci. Acad., Part A* **55,** 721 (1989).
36. L. Néel, *Ann. Phys.* **3,** 139 (1948).
37. K. Tkáčová, V. Šepelák, N. Števulová, and V. V. Boldyrev, *J. Solid State Chem.* **123,** 100 (1996).
38. V. Šepelák, K. Tkáčová, and A. I. Rykov, *Cryst. Res. Technol.* **28,** 53 (1993).
39. V. Šepelák and J. Rodriguez-Carvajal. [unpublished results]
40. T. Sato, K. Haneda, M. Seki, and T. Iijima, *in* "Proceedings of the International Symposium on Physics of Magnetic Materials," p. 210. World Scientific, Singapore, 1987.
41. T. Sato, K. Haneda, M. Seki, and T. Iijima, *Appl. Phys. A* **50,** 13 (1990).
42. T. Kamiyama, K. Haneda, T. Sato, S. Ikeda, and H. Asano, *Solid State Commun.* **81,** 563 (1992).